

GWADW: May 21-27, 2023
Hotel Hermitage, La Biodola, Isola d'Elba

Forecasting the Detection and Parameter Estimation Capabilities for different ET Designs

Ulyana Dupletsa

on behalf of

Branchesi, Maggiore et al. (arXiv:2303.15923)



Science with the Einstein Telescope: a comparison of different designs

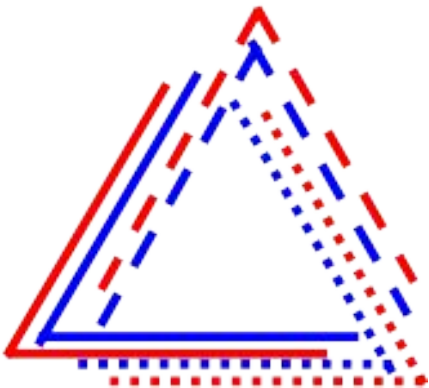
Marica Branchesi,^{1,2} Michele Maggiore,^{3,4} David Alonso,⁵ Charles Badger,⁶ Biswajit Banerjee,^{1,2} Freija Beirnaert,⁷ Swetha Bhagwat,^{8,9} Marie-Anne Bizouard,¹⁰ Guillaume Boileau,^{11,10} Ssohrab Borhanian,¹² Daniel David Brown,¹³ Man Leong Chan,¹⁴ Nelson Christensen,¹⁰ Giulia Cusin,^{15,3,4} Stefan L. Danilishin,^{16,17} Jerome Degallaix,¹⁸ Valerio De Luca,¹⁹ Arnab Dhani,²⁰ Tim Dietrich,^{21,22} Ulyana Dupletsa,^{1,2} Stefano Foffa,^{3,4} Gabriele Franciolini,⁸ Andreas Freise,^{23,16} Gianluca Gemme,²⁴ Boris Goncharov,^{1,2} Archisman Ghosh,⁷ Francesca Gulminelli,²⁵ Ish Gupta,²⁰ Pawan Kumar Gupta,^{16,26} Jan Harms,^{1,2} Nandini Hazra,^{1,2,27} Stefan Hild,^{16,17} Tanja Hinderer,²⁸ Ik Siong Heng,²⁹ Francesco Iacovelli,^{3,4} Justin Janquart,^{16,26} Kamiel Janssens,^{10,11} Alexander C. Jenkins,³⁰ Chinmay Kalaghatgi,^{16,26,31} Xhesika Korovesi,^{32,33} Tjonnie G. F. Li,^{34,35} Yufeng Li,³⁶ Eleonora Loffredo,^{1,2} Elisa Maggio,²² Michele Mancarella,^{3,4,37,38} Michela Mapelli,^{39,40,41} Katarina Martinovic,⁶ Andrea Maselli,^{1,2} Patrick Meyers,⁴² Andrew L. Miller,^{43,16,26} Chiranjib Mondal,²⁵ Niccolò Muttoni,^{3,4} Harsh Narola,^{16,26} Micaela Oertel,⁴⁴ Gor Oganessian,^{1,2} Costantino Pacilio,^{8,37,38} Cristiano Palomba,⁴⁵ Paolo Pani,⁸ Antonio Pasqualetti,⁴⁶ Albino Perego,^{47,48} Carole Pérois,^{39,40,41} Mauro Pieroni,^{49,50} Ornella Juliana Piccinni,⁵¹ Anna Puecher,^{16,26} Paola Puppo,⁴⁵ Angelo Ricciardone,^{52,39,40} Antonio Riotto,^{3,4} Samuele Ronchini,^{1,2} Mairi Sakellariadou,⁶ Anuradha Samajdar,²¹ Filippo Santoliquido,^{39,40,41} B.S. Sathyaprakash,^{20,53,54} Jessica Steinlechner,^{16,17} Sebastian Steinlechner,^{16,17} Andrei Utina,^{16,17} Chris Van Den Broeck,^{16,26} and Teng Zhang^{9,17}

Science Reference Paper for the CoBA study

Work coordinated by
Marica Branchesi and
Michele Maggiore

submitted to JCAP

Reference Design of ET



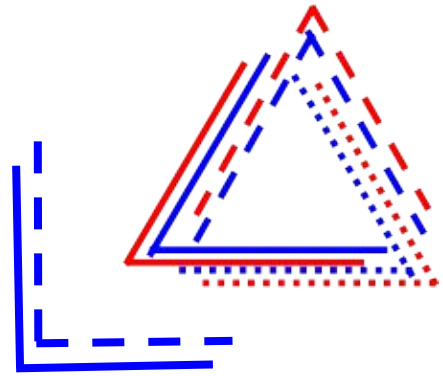
The reference ET configuration consists of:

- **Triangular** shape
- **10 km** arms
- 3 nested detectors in xylophone configuration: **HF + LF** (cryogenic)

Different Configurations

We want to evaluate the effect on the **Science Case** of:

- Changes in geometry: triangle vs 2L, different arm lengths
- Role of the low frequency instrument: what happens if we have only the HF part?



- Triangle, 10 km arms
(reference design)
- 2L, 15 km arms, parallel
- 2L, 15 km arms, at 45°
- Triangle, 15 km arms
- 2L, 20 km arms, parallel
- 2L, 20 km arms, at 45°

Fisher Matrix Analysis

gwbench

S. Borhanian, 2021,
Class.Quant.Grav.

[GitLab link](#)



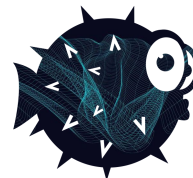
GWFAST

F. Iacovelli,
M. Mancarella, et al.
2022, *Astrophys.J.*

[GitHub link](#)

TiDoFM

Li et al.
2022, *Phys. Rev. D*



GWFISH

GWFish

U. Dupletsa, J. Harms,
et al.
2023, *Astronomy and
Computing*

[GitHub link](#)

Starting Assumptions

- We use waveform including higher order modes and tidal deformability parameters (for BNSs): **IMRPhenomXPHM** and **IMRPhenomD_NRTidalv2**
- The parameters of the waveform are:

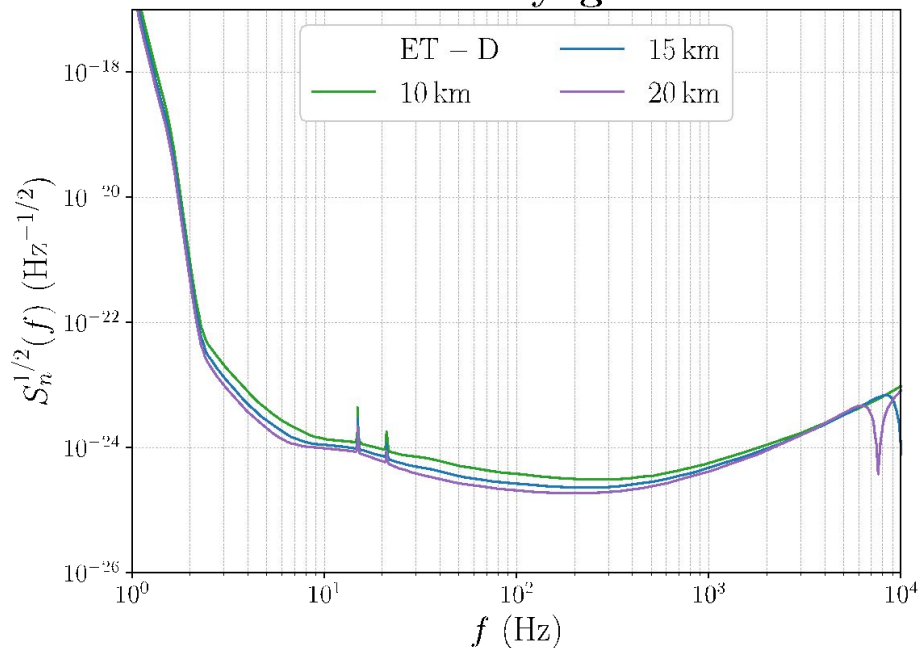
$$\{\mathcal{M}_c, \eta, d_L, \underbrace{\theta, \phi}_{\text{sky position}}, \iota, \psi, t_c, \Phi_c, \underbrace{\chi_{1,x}, \chi_{2,x}, \chi_{1,y}, \chi_{2,y}, \chi_{1,z}, \chi_{2,z}}_{\text{spin parameters}}, \underbrace{\Lambda_1, \Lambda_2}_{\text{tidal polarizability (for BNSs only)}}\}.$$

- The BNS population was obtained using **MOBSE** (isolated binaries) with a local merger rate of $250 \text{ Gpc}^{-3} \text{ yr}^{-1}$ (to compare to the LVK result of $10\text{-}1700 \text{ Gpc}^{-3} \text{ yr}^{-1}$)
- The BBH population was obtained using **FASTCLUSTER** (isolated evolution + dynamical formation channel)

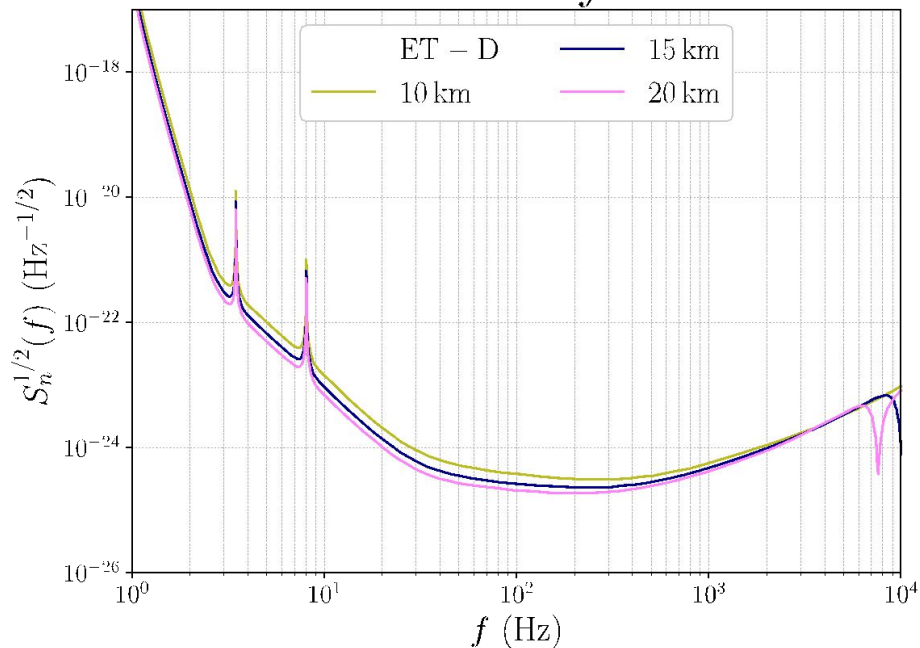
Sensitivity Curves (provided by the ISB)

Actual curves are still evolving!

HFLF cryogenic



HF only



Structure of the Work

Contents

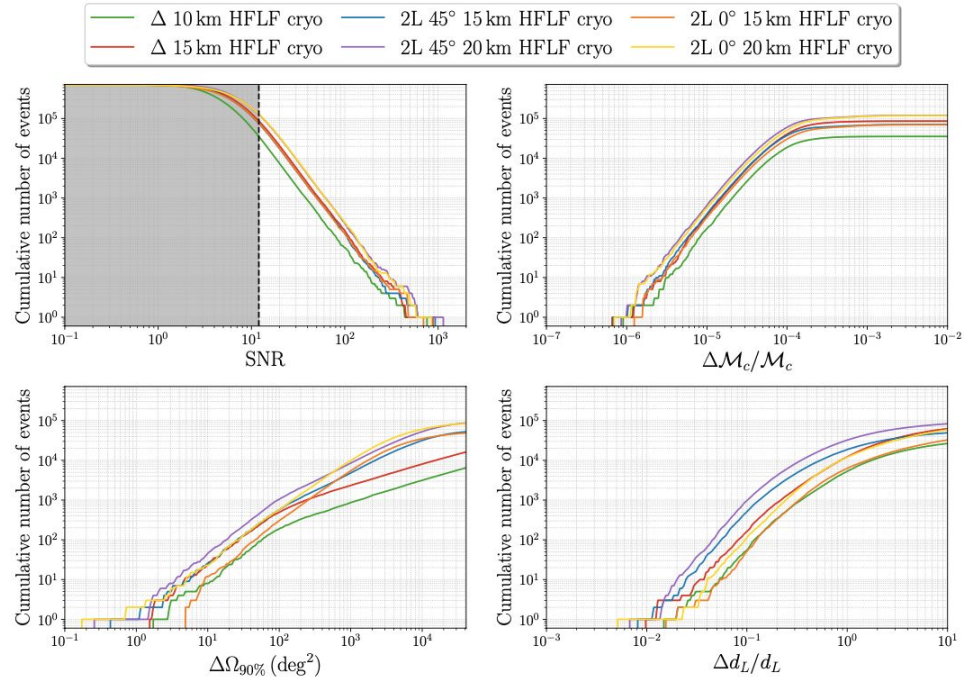
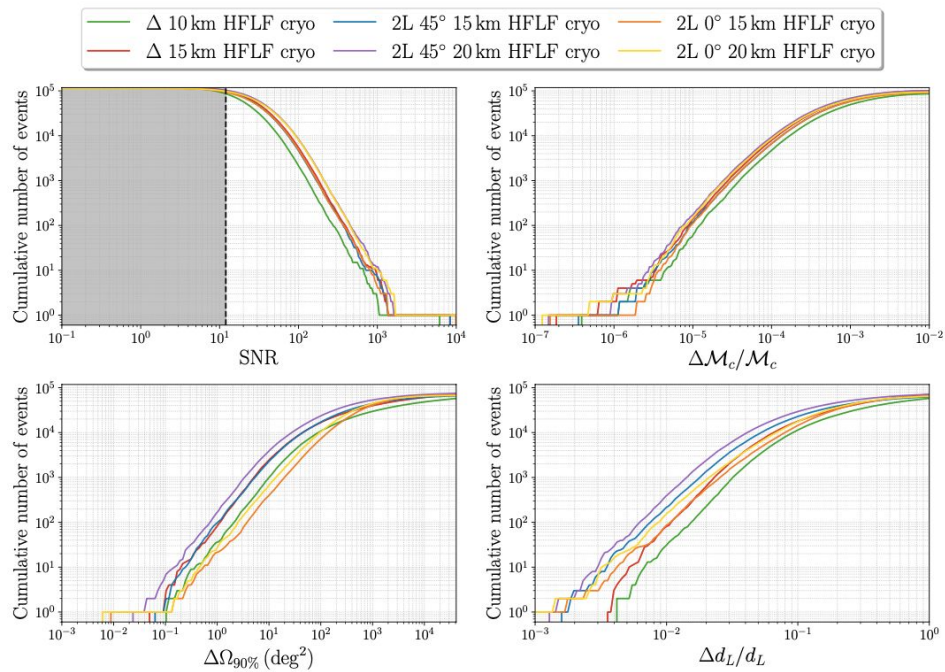
1	Introduction	1
2	Detector geometries and sensitivity curves	4
3	Coalescence of compact binaries	9
3.1	Binary Black Holes	11
3.1.1	Comparison between geometries	11
3.1.2	Effects of a change in the ASD	13
3.1.3	Golden events	15
3.2	Binary Neutron Stars	23
3.2.1	Comparison between geometries	23
3.2.2	Effects of a change in the ASD	23
3.2.3	Golden events	24
3.2.4	Dependence on the population model	25
3.3	ET in a network of 3G detectors	34
4	Multi-messenger astrophysics	39
4.1	BNS sky-localization and pre-merger alerts	39
4.2	Gamma-ray bursts: joint GW and high-energy detections	43
4.2.1	Prompt emission	44
4.2.2	Afterglow: survey and pointing modes	45
4.3	Kilonovae: joint GW and optical detections	48
5	Stochastic backgrounds	51
5.1	Sensitivity to isotropic stochastic backgrounds	53
5.2	Angular sensitivity	55
5.3	Astrophysical backgrounds	57
5.4	Impact of correlated magnetic, seismic and Newtonian noise	59
5.4.1	Seismic and Newtonian Noise	60
5.4.2	Magnetic noise	63
6	Impacts of detector designs on specific science cases	68
6.1	Physics near the BH horizon	68
6.1.1	Testing the GR predictions for space-time dynamics near the horizon	68
6.1.2	Searching for echoes and near-horizon structures	72
6.1.3	Constraining tidal effects and multipolar structure	74
6.2	Nuclear physics	76
6.2.1	Radius estimation from Fisher-matrix computation	76
6.2.2	Full parameter estimation results	80
6.2.3	Connected uncertainty of nuclear-physics parameters	81
6.2.4	Postmerger detectability	83
6.2.5	Conclusions: nuclear physics with ET	85
6.3	Population studies	85
6.3.1	Merger rate reconstruction	85
6.3.2	Constraints on PBHs from high-redshift mergers	88
6.3.3	Other PBH signatures	91
6.4	Cosmology	94
6.4.1	Hubble parameter and dark energy from joint GW/EM detections	94
6.4.2	Hubble parameter and dark energy from BNS tidal deformability	106
6.4.3	Hubble parameter from high-mass ratio events	108
6.5	Cosmological stochastic backgrounds	113
6.5.1	Cosmic Strings	113
6.5.2	First-order phase transition	114
6.5.3	Source separation	116
6.6	Continuous waves	117
6.6.1	CWs from spinning neutron stars	118
6.6.2	Transient CWs	122
6.6.3	Search for dark matter with CWs	124
6.6.4	Conclusions	126
7	The role of the null stream in the triangle-2L comparison	127

Coalescence of Compact Binaries

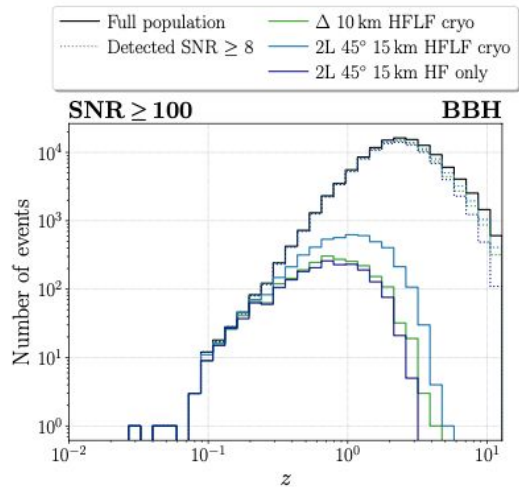
1 year of observations!

BBH

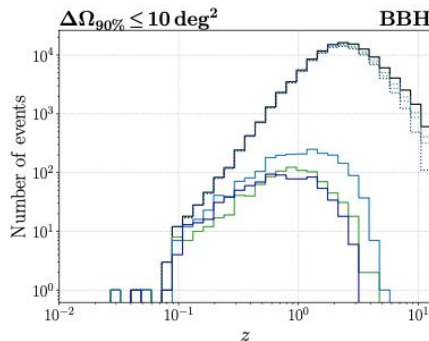
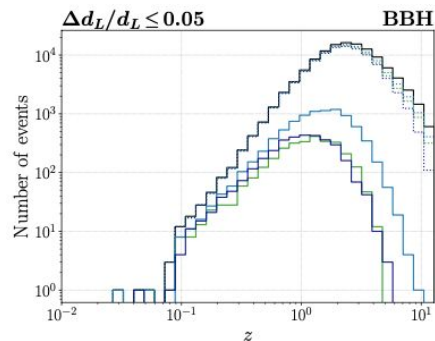
BNS



Coalescence of Compact Binaries: Golden Events



Configuration	SNR ≥ 100
Δ -10km-HFLF-Cryo	2298
Δ -15km-HFLF-Cryo	5730
2L-15km-45°-HFLF-Cryo	4933
2L-20km-45°-HFLF-Cryo	8828
2L-15km-0°-HFLF-Cryo	5143
2L-20km-0°-HFLF-Cryo	8551
2L-15km-45°-HF	1987



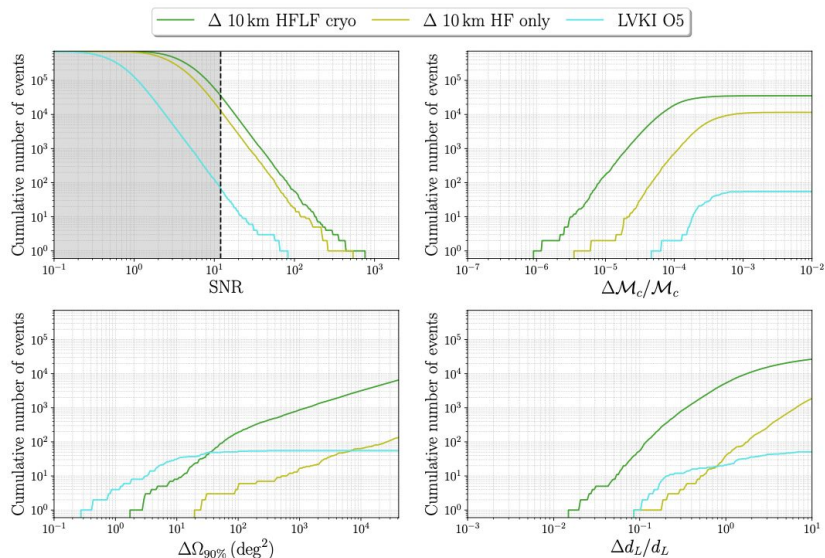
The full population contains
 1.2×10^5 BBH events!

Coalescence of Compact Binaries

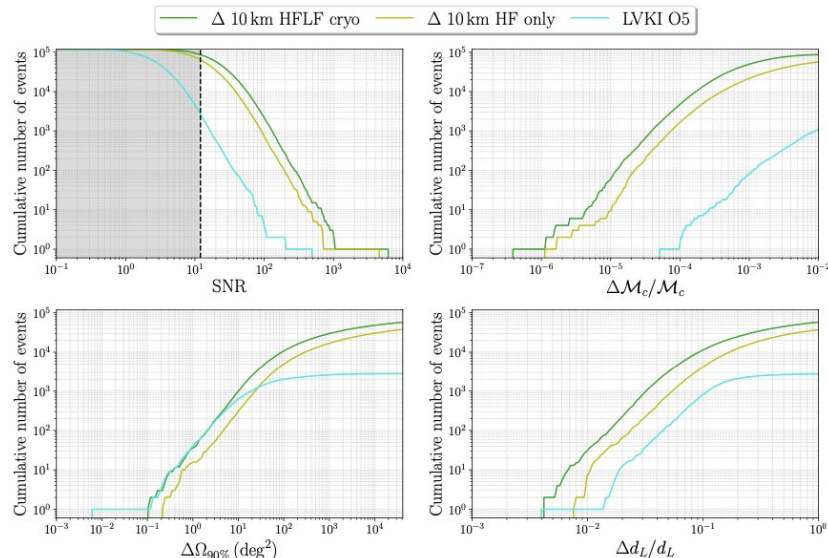
- The reference design of 10 km has remarkable performance, improving by orders of magnitude with respect to 2G
- The 2L-15 km-45° configuration improves by a further factor of 2-3, especially for distance and sky localization
- The 2L-15km-0° configuration is disfavored, because of the poor angular localization capabilities

Coalescence of Compact Binaries: losing LF

BNS



BBH



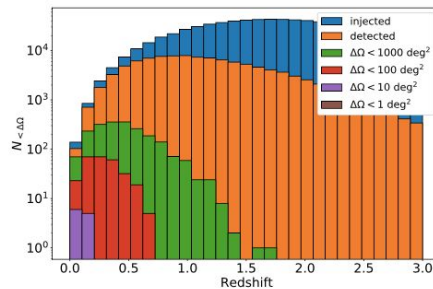
- LF sensitivity is particularly important for BNSs as they stay for a longer time in bandwidth
- The reference triangle-10 km design is well superior LVK-O5 even if we have only HF sensitivity, except for angular localization

Multi-Messenger Astronomy

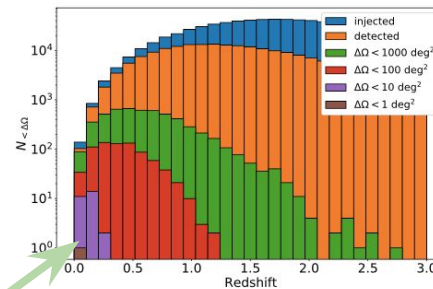
The key parameters to take into account are:

- Ability to localize the source
- Number of joint detections (SNR > 8)
- Reached redshift
- Pre-merger detection and parameter estimation

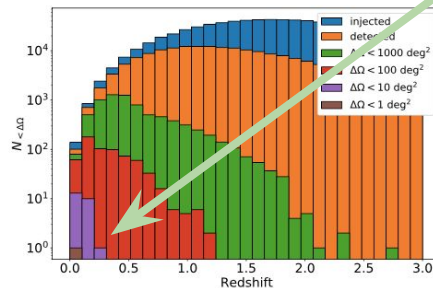
The 2L-15km-45° is comparable to Δ -15km and is better than Δ -10km



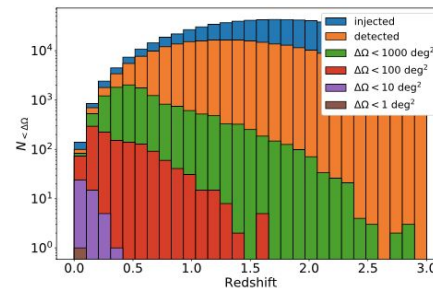
(a) Δ 10 km HFLF cryo



(b) Δ 15 km HFLF cryo



(d) 2L 15 km HFLF cryo



(e) 2L 20 km HFLF cryo

Multi-Messenger Astronomy: HF only

Full (HFLF cryo) sensitivity detectors

$\Delta\Omega_{90\%}(\text{deg}^2)$	All orientation BNSs				BNSs with viewing angle $\Theta_v < 15^\circ$			
	$\Delta 10$	$\Delta 15$	2L 15	2L 20	$\Delta 10$	$\Delta 15$	2L 15	2L 20
10	11	27	24	45	0	1	2	5
40	78	215	162	350	8	22	20	33
100	280	764	644	1282	26	74	68	133
1000	2112	5441	7478	13482	272	632	1045	1725

on-axis events

HF sensitivity detectors

$\Delta\Omega_{90\%}(\text{deg}^2)$	All orientation BNSs				BNSs with viewing angle $\Theta_v < 15^\circ$			
	$\Delta 10$	$\Delta 15$	2L 15	2L 20	$\Delta 10$	$\Delta 15$	2L 15	2L 20
10	0	1	5	5	0	0	2	2
40	4	10	20	47	0	5	6	17
100	14	53	76	144	7	33	35	64
1000	145	548	1662	3378	80	336	672	1302

- Significantly smaller number of well-localized events ($<100\text{deg}^2$), especially for the Δ -configurations
- For the on-axis events the percentage decrease of well-localized events is smaller than that for randomly oriented events
- 2L-15km-HF and 2L-20km-HF are worse than Δ -10km-cryo for randomly oriented systems
- 2L-15km-HF is comparable to the full Δ -10km-cryo for on-axis events

Multi-Messenger Astronomy: Pre-Merger Detections

Full (HFLF cryo) sensitivity detectors

Configuration	$\Delta\Omega_{90\%}$	All orientation BNSs			BNSs with $\Theta_v < 15^\circ$		
	[deg ²]	30 min	10 min	1 min	30 min	10 min	1 min
$\Delta 10\text{km}$	10	0	1	5	0	0	0
	100	10	39	113	2	8	20
	1000	85	293	819	10	34	132
	All detected	905	4343	23597	81	393	2312
$\Delta 15\text{km}$	10	1	5	11	0	1	1
	100	41	109	281	6	14	36
	1000	279	806	2007	33	102	295
	All detected	2489	11303	48127	221	1009	4024
2L 15 km misaligned	10	0	1	8	0	0	0
	100	20	54	169	2	7	26
	1000	194	565	1399	23	73	199
	All detected	2172	9598	39499	198	863	3432
2L 20 km misaligned	10	2	4	15	1	1	2
	100	39	118	288	7	19	47
	1000	403	1040	2427	47	128	346
	All detected	4125	17294	56611	363	1588	4377

Detections
within $z=1.5$

Pre-merger detections are critical to detect the prompt/early multi-wavelength emission in order to:

- Probe the central engine of GRBs, and in particular to understand the jet composition, the particle acceleration mechanism, the radiation and energy dissipation mechanisms (VHE prompt CTA/ET synergy - see **Banerjee et al., 2023**)
- To probe the structure of the outer sub-relativistic ejecta, early UV emission (ULTRASAT/UVEX/DORADO synergy)

Similar performances for on-axis events!

Without LF

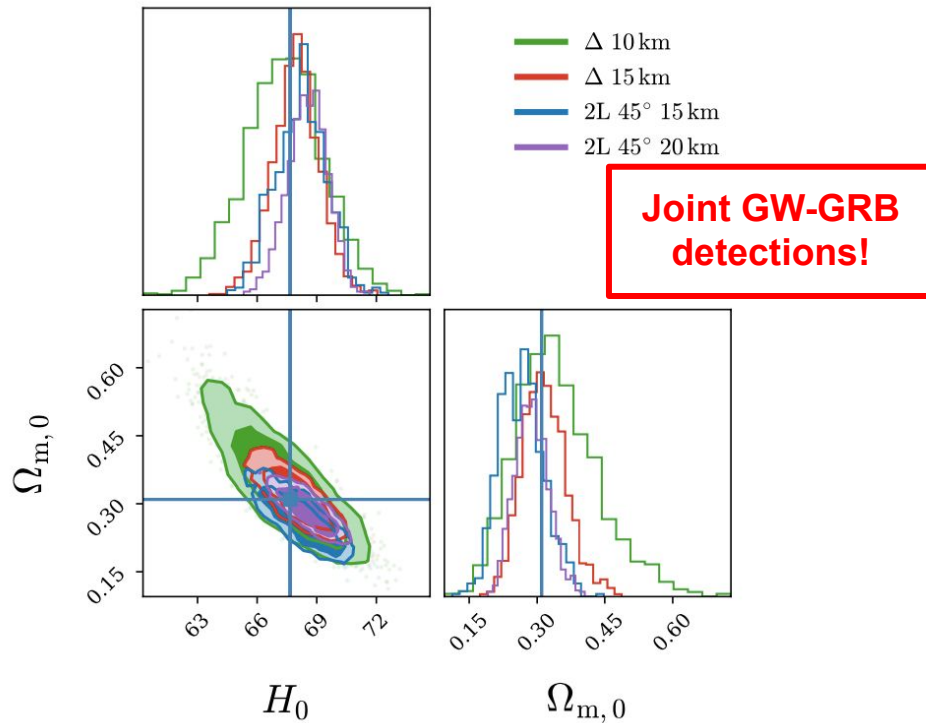
HF sensitivity detectors

Configuration	$\Delta\Omega_{90\%}$	All orientation BNSs			BNSs with $\Theta_v < 15^\circ$		
	[deg ²]	30 min	10 min	1 min	30 min	10 min	1 min
$\Delta 10\text{km}$	100	0	0	0	0	0	0
	1000	0	0	4	0	0	1
	All detected	0	3	317	0	0	26
$\Delta 15\text{km}$	100	0	0	2	0	0	0
	1000	0	0	10	0	0	4
	All detected	2	8	891	0	1	84
2L 15 km misaligned	100	0	0	0	0	0	0
	1000	0	0	7	0	0	3
	All detected	0	7	743	0	1	69
2L 20 km misaligned	100	0	0	3	0	0	0
	1000	0	0	13	0	0	6
	All detected	2	11	1535	0	1	146

Detections
within $z=1.5$

**No localized
pre-merger
detections!**

Cosmology: ET + THESEUS



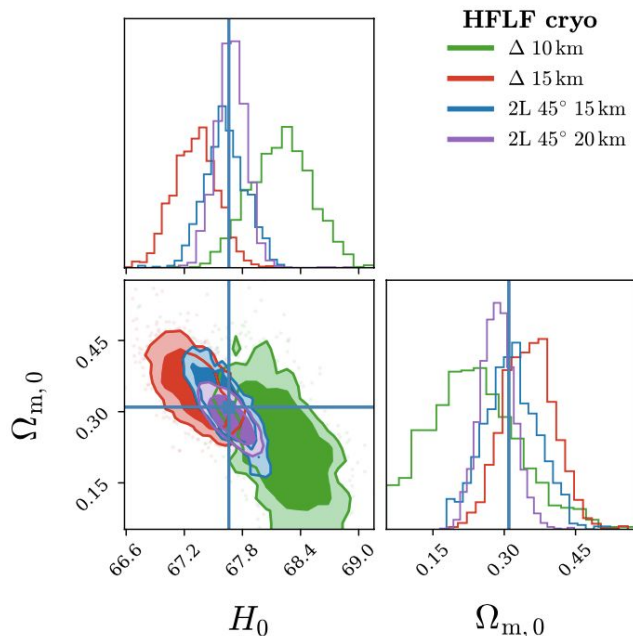
- 5 years of observations
- **75 joint detections** in the configuration 2L-20km-cryo
- Solid and conservative results based on prompt GRB observations

Configuration	$\Delta H_0/H_0$	$\Delta \Omega_M/\Omega_M$
Δ -10km	0.057	0.546
Δ -15km	0.035	0.290
2L-15km- 45°	0.040	0.370
2L-20km- 45°	0.029	0.276

Cosmology: ET + VRO

Joint GW-kilonova
detections

- 1 year of observations
(larger number of joint detections expected)
- **115 joint detections**
for 2L-20km-cryo
- Dependence on BNS
merger rate
normalization

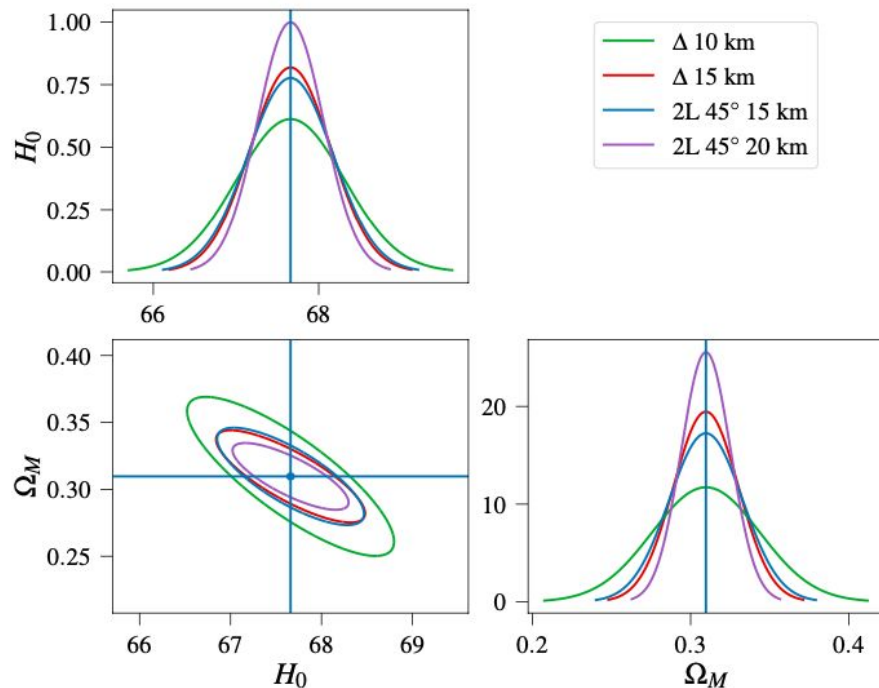


HFLF cryogenic		
Configuration	$\Delta H_0/H_0$	$\Delta \Omega_M/\Omega_M$
Δ-10km	0.009	0.832
Δ-15km	0.007	0.303
2L-15km-45°	0.006	0.370
2L-20km-45°	0.004	0.243

HF only		
Configuration	$\Delta H_0/H_0$	$\Delta \Omega_M/\Omega_M$
Δ-10km	0.065	1.23
Δ-15km	0.057	1.86
2L-15km-45°	0.066	1.31
2L-20km-45°	0.031	1.22

Dramatic reduction of joint detections
without LF in both cases!

Cosmology from BNS Tidal Deformability



- Assuming that the nuclear EOS is known
- The source-frame mass can be determined from the measurement of tidal deformability
- Direct measurement of z from the GW signal
- Sub-percent error on H_0 with a single year of observing run with ET alone

Configuration	$\Delta H_0/H_0$	$\Delta \Omega_M/\Omega_M$
Δ -10km	9.63×10^{-3}	1.10×10^{-1}
Δ -15km	7.20×10^{-3}	6.62×10^{-2}
2L-15km-45°	7.59×10^{-3}	7.47×10^{-2}
2L-20km-45°	5.90×10^{-3}	5.04×10^{-2}

CoBA Conclusions

- All the triangular and 2L geometries that have been investigated can be the baseline of a **superb 3G detector**, that will allow to improve by orders of magnitude compared to 2G detectors
- The **2L-15km-45° configuration** in general offer a better scientific return with respect to the Δ -10km, and has a similar performance on all parameters (for both BBHs and BNSs) to the **Δ -15km**
- The **low frequency sensitivity** is crucial for exploiting the full potential of ET. In the HF-configuration only, independently of the chosen geometry, several scientific targets would be lost or significantly diminished

Thank you!

